



Visingardi, A. et al. (2017) Forces on Obstacles in Rotor Wake – A GARTEUR Action Group. In: 43rd European Rotorcraft Forum, Milan, Italy, 12-15 Sep 2017

This is the author's final accepted version.

There may be differences between this version and the published version. You are advised to consult the publisher's version if you wish to cite from it.

<http://eprints.gla.ac.uk/148663/>

Deposited on: 22 September 2017

Enlighten – Research publications by members of the University of Glasgow
<http://eprints.gla.ac.uk>

FORCES ON OBSTACLES IN ROTOR WAKE – A GARTEUR ACTION GROUP

Antonio Visingardi, a.visingardi@cira.it, CIRA (Italy)
Fabrizio De Gregorio, f.degregorio@cira.it, CIRA (Italy)
Thorsten Schwarz, thorsten.schwarz@dlr.de, DLR (Germany)
Matthias Schmid, matthias.schmid@dlr.de, DLR (Germany)
Richard Bakker, rbakker@nlr.nl, NLR (The Netherlands)
Spyros Voutsinas, spyros@fluid.mech.ntua.gr, NTUA (Greece)
Quentin Gallas, quentin.gallas@onera.fr, ONERA (France)
Ronan Boisard, ronan.boisard@onera.fr, ONERA (France)
Giuseppe Gibertini, giuseppe.gibertini@polimi.it, Politecnico di Milano (Italy)
Daniele Zagaglia, daniele.zagaglia@polimi.it, Politecnico di Milano (Italy)
George Barakos, g.barakos@glasgow.ac.uk, University of Glasgow (United Kingdom)
Richard Green, richard.green@glasgow.ac.uk, University of Glasgow (United Kingdom)
Giulia Chirico, g.chirico.1@research.gla.ac.uk, University of Glasgow (United Kingdom)
Michea Giuni, michea.giuni@glasgow.ac.uk, University of Glasgow (United Kingdom)

Abstract

The paper describes the objectives and the structure of the GARTEUR Action Group HC/AG-22 project which deals with the basic research about the forces acting on obstacles when immersed in rotor wakes. The motivation started from the observation that there was a lack of experimental databases including the evaluation of the forces on obstacles in rotor wakes; and of both numerical and experimental investigations of the rotor downwash effects at medium-to-high separation distances from the rotor, in presence or without sling load. The four research centres: CIRA (I); DLR (D); NLR (NL); ONERA (F); and three universities: NTUA (GR); Politecnico di Milano (I); University of Glasgow (UK) created a team for the promotion of activities that could contribute to fill these gaps. In particular, both numerical and experimental investigations were proposed by the team to study, primarily, the effects of the confined area geometry on a hovering helicopter rotor, and, secondarily, the downwash and its influence on the forces acting on a load, loose or slung, at low to high separation distances from the rotor disc. The following activities were planned: a) application and possible improvement of computational tools for the study of helicopter rotor wake interactions with obstacles; b) set-up and performance of four cost-effective wind tunnel test campaigns aimed at producing a valuable experimental database for the validation of the numerical methodologies applied; c) final validation of the numerical methodologies. The project started in November 2014 and has a duration of three years.

1 NOMENCLATURE

Symbol	Description	Units
c	Chord length	m
C_p	Pressure coefficient	
Ω	Rotor speed	RPM
D	Rotor diameter	m
R	Rotor radius	m
u, v, w	Velocity components	m/s
x, y, z	Geometrical coordinates	m
Δp	Pressure difference wrt p_∞	Pa
Θ_0	Collective pitch	deg
μ	Advance ratio	
σ	Rotor solidity	
HIGE	Hover In Ground Effect	
HOGE	Hover Out of Ground Effect	

2 INTRODUCTION

A helicopter is an aircraft that generates the lifting force by means of the blades, which are rotating aerodynamic surfaces. Therefore, a helicopter does not necessarily require a relative wind to fly and can efficiently operate in

hover or low-speed forward flight, in contrast to fixed-wing aircraft. These are the main reasons why helicopters are employed in missions within “confined areas”.

A confined area is a region where the flight of the helicopter is limited in some direction by terrain or by the presence of obstacles, natural or manmade, such as steep valleys and buildings. Rescue operations, emergency medical services, ship-based rotorcraft operations are just some examples of helicopter missions within confined areas, Figure 1.



Figure 1: Examples of helicopter operations in confined areas

The wake system generated by the helicopter rotor may interact with the airflow around the obstacles, with an intensity that increases with the proximity of the rotor to the ground and/or the obstacles. This mutual interaction generates aerodynamic forces that may result in: (a) high compensatory workload for the pilot; (b) degradation of the handling qualities and performance of the aircraft; (c) unsteady forces on the structure of the surrounding obstacles; (d) noise levels creating discomfort to the community residing in the area.

The obstacle wake can be highly unsteady, complex and challenging to predict, Figure 2.

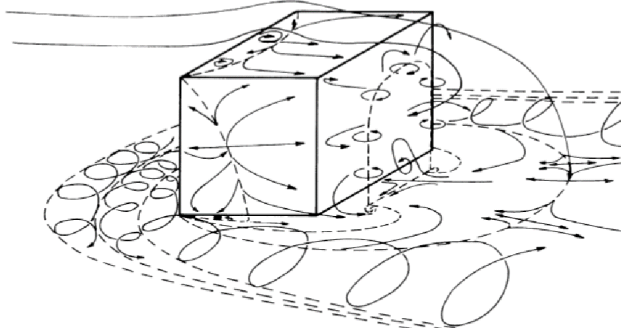


Figure 2: Complexity of the obstacle wake^[1.]

This flowfield is further complicated by the presence of the helicopter which induces an additional flowfield that can significantly alter the upstream airflow when the aircraft is operating close to a surface. Thus, the helicopter experiences a combination of the wake induced by the obstacle and the airflow induced by itself.

The presence of vertical surfaces forces a part of the rotor wake to flow upward along the walls and to become the recirculatory inflow with respect to the rotor, Figure 3. The aerodynamic performance of the rotor changes because the upward rotor wake interferes with the flow field around the rotor.

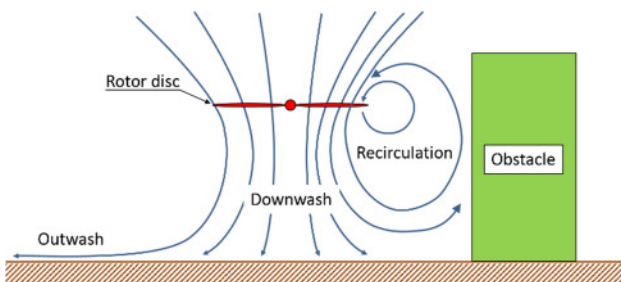


Figure 3: Helicopter operations in confined areas

A helicopter sling load, Figure 4, is another, yet particular, case of obstacle subjected to forces produced by its interaction with the rotor wake. Once airborne a sling load comes under the influence of aerodynamic forces and moments associated with its size, shape, mass, and transport speed. Furthermore, in the particular case of hover/low-speed forward flight conditions, where the load is fully immersed in the rotor wake system, these forces are strongly related to the intensity of the downwash effects of the wake which, in turn, are mainly dependent on the blade

loading and on the distance of the sling load from the rotor disc. The instabilities that can arise from these forces affect the rotorcraft and/or the load itself, and their avoidance is therefore crucial not only for safety reasons but also when a controlled attitude of the load is required. An example for the latter case is represented by drop test experiments, such as PHOENIX^[2.], NASA X40-A^{[3.],[4.]}, ESA-IXV^[5.], in which the helicopter is both the carrier and the launch station of tests articles, which represent the sling load, Figure 5.



Figure 4: Helicopter with a sling load



Figure 5: NASA X40-A drop test^[4.]

2.1 Previous work

Several publications address the problem of the helicopter ground effect in confined areas and the majority of them concern investigations of the helicopter-ship interactional problem, example papers are reported in references^{[6.],[11.]}, whereas a numerical and experimental investigation concerning the more general problem of the rotor performance in the wake of a large structure is illustrated in Quinliven^[12.]. Nevertheless, references of the evaluation of forces acting on obstacles in rotor wake are scarce. Likewise, there are few experimental databases for the validation of numerical methodologies, their accessibility is uncertain, and do not provide force measurements on obstacle surfaces.

A few papers describe the characteristics of some experimental databases. They also testify the complexity of the problem and the importance to better understand the phenomenology and its implication on the flight safety. Some relevant examples are provided in the following:

- a pioneering work is represented by Timm^[13.] in which the author illustrates the basic requirements for the generation of an obstacle-induced flow recirculation and what the driving parameters are. Qualitative results of an experimental activity are provided and solutions for a mitigation of the problem are also proposed;
- a more recent experimental investigation is illustrated in Iboshi^[14.]. The authors illustrate the set-up of an experiment consisting in a rotor hovering over a ground plate delimited by one or two vertical plates. Performance evaluations are made at certain combinations of the wall height, space between walls and rotor height. An increase in the required torque

coefficient as well as in the vibratory torque coefficient is produced by the presence of the vertical walls;

- the comparisons of Navier-Stokes CFD predictions of the airflow around a helicopter rotor hovering near a land-based hangar with experimental velocity data gathered during a flight test campaign by using ultrasonic anemometers are illustrated in Polsky^[15]. The rotor is numerically modelled by an actuator disk and several turbulence models are tested. The importance of an atmospheric boundary layer (ABL) modelling is also considered. Although the helicopter downwash dominates the flowfield, the CFD investigation also demonstrates the importance of accurately predicting the flow over and around the hangar structure. For this purpose, experimental data were gathered by the authors around the full scale hangar and sub-scale wind tunnel data including surface pressures and oil flow but these results are not shown in the paper;
- the occurrence of aerodynamic interference between a helicopter and obstacles of different shapes located in the vicinity of the helicopter is numerically and experimentally investigated in Lusiak^[16]. For the particular case of a well-shaped obstacle, such as a typical town courtyard, numerical computations are performed by coupling the FLUENT software for the rotor aerodynamics with a panel code for the fuselage aerodynamics and compared with the measurements made in a low turbulence wind tunnel TMT in terms of tensometric measurements of forces and moments. The results indicate that the phenomenon of aerodynamic interference can seriously disturb the flow around the helicopter and change the loading of some of its elements. Substantial changes in the value of the resulting loads can make the helicopter difficult to control.

The aerodynamics of helicopter slung-load systems is investigated in a few publications. A relevant example is given by Gabel^[17], where a specific section is dedicated to the experimental evaluation of the aerodynamic instabilities induced by the load attitude and the separation distance of the load from the helicopter. CFD is used in Prosser^[18] to resolve the unsteady Navier-Stokes equations for prediction of aerodynamic forces and moments acting on dynamic helicopter sling loads; no influence of the rotor wake is taken into account. Similarly, Theron^[19] summarizes the work on the aerodynamics of a slung load cargo container without considering the effect of the rotor wake: two different CFD codes are used to study the three-dimensional flow over the stationary container and the two-dimensional simulation of the stationary and oscillating container. Comparisons with experimental measurements are also reported. Finally, two relevant papers concerning the measurement of the helicopter downwash velocity are represented by Leese^{[20],[21]}, where no sling load is however considered.

2.2 Objectives

The analysis of the previous work highlights the lack of experimental databases including the evaluation of the forces acting on obstacles when immersed in rotor wakes. Instead, in the case of the helicopter sling-load problem, the lack of both numerical and experimental investigations of the rotor downwash effect at medium-to-high separation

distances from the rotor, in presence or without sling load, is observed.

An Action Group, namely HC/AG-22^[22], was created in the framework of the GARTEUR organization by four research centres: CIRA (I); DLR (D); NLR (NL); ONERA (F) and three universities: NTUA (GR); Politecnico di Milano (I) - PoliMi; University of Glasgow (UK) - UoG, with the aim to promote activities which could contribute to fill these gaps. For the purpose, this team proposed to investigate, both numerically and experimentally:

- primarily, the effects of the confined area geometry on a hovering helicopter rotor from the standpoints of both the phenomenological understanding of the interactional process and the evaluation of the forces acting on surrounding obstacles;
- secondarily, the downwash and its influence on the forces acting on a load, loose or slung, at low to high separation distances from the rotor disc.

The know-how acquired by the GARTEUR AG-17^{[23],[24]} about the wake modelling in the presence of ground obstacles was capitalised and set-up the basis for this new research activity.

The project, started in November 2014, has a duration of three years, with conclusion planned for October 2017, during which the following activities are planned:

- application and possible improvement of computational tools for the study of helicopter rotor wake interactions with obstacles;
- set-up and performance of cost-effective wind tunnel test campaigns aimed at producing a valuable experimental database for the validation of the numerical methodologies applied;
- final validation of the numerical methodologies.

The present paper provides the details of the above indicated activities. In particular, section 3 illustrates the statement of the work. The wind tunnel experiments and the numerical activities are described, together with some example of results obtained, in sections 4 and 5, respectively. Some conclusions are finally drawn in section 6.

3 STATEMENT OF WORK

In order to achieve the objectives of HC/AG-22, the project is structured in four work packages. The partners are involved in experimental activities, during which suitable databases are produced for the phenomenological understanding and the quantification of the forces arising during the rotor-ground-obstacles interactional process, as well as numerical activities aimed at both providing baseline indications for the set-up of the experiments, and enhancing and validating the employed commercial or in-house computational tools.

3.1 Project Work Package Architecture

The project architecture is shown in Figure 6 and a short description of the work packages is provided in the following.

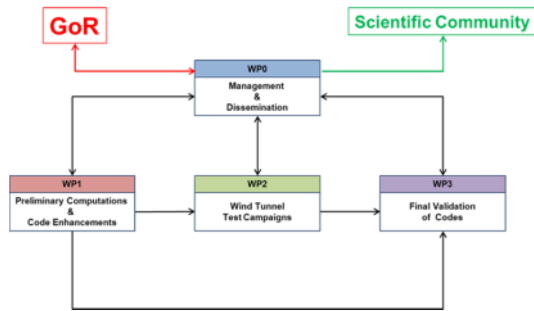


Figure 6: Project work package architecture

- **WP0 – Management & Dissemination:** is aimed at the fulfilment of all the obligations concerning the project management and the dissemination of the results. Through this work package the project interacts with: the Group of Responsables (GoR), by receiving inputs and providing the information required; and the scientific community, by collecting the results of the activities of the other three work packages and disseminating them;
- **WP1 – Preliminary Computations & Code Enhancements:** deals with a preparation phase during which partners are involved in literature review and computational activities aimed at providing necessary and useful inputs to the two following work packages where experimental databases are produced (WP2) and the modelling capabilities of the applied numerical tools are validated (WP3). It also provides WP0 with all the information required for management and dissemination;
- **WP2 – Wind Tunnel Test Campaigns:** concerns the performance of four wind tunnel test campaigns that have been identified by partners as particularly meaningful for the phenomenological understanding of the flow field generated by a model rotor operating in HOGE/HIGE conditions in the presence of obstacles, and the quantification of the forces acting on them. The resulting experimental databases are used in WP3 for the final validation of the numerical tools proposed by the partners. It also provides WP0 with all the information required for management and dissemination;
- **WP3 – Final Validation of Codes:** is aimed at the final validation of the numerical tools proposed by partners. The validation is performed by comparing the numerical results of the computational activity with the experimental data produced during the wind tunnel test campaigns of the project in the framework of WP2. The work package also provides WP0 with all the information required for management and dissemination.

4 WIND TUNNEL EXPERIMENTAL ACTIVITIES

The four partners CIRA, ONERA, PoliMi and UoG proposed four different wind tunnel test campaigns, complementary to each other, to be carried out in their own wind tunnel facilities and aiming at analysing, with a wider and deeper insight, different aspects of the phenomenology. A fully instrumented obstacle was put at disposal by DLR.

Table 1 reports a summary of these experiments, while the main characteristics of the test rigs, of the wind tunnels, and of the model obstacle are illustrated in the following.

PARTNER	EXPERIMENT DESCRIPTION	MEASUREMENTS
CIRA	HOGE/HIGE rotor with a loose/sling load	Rotor thrust and induced loads on the obstacle. Steady and unsteady pressures on the obstacle. PIV measurements
ONERA	HIGE rotor in proximity to a well-shaped obstacle	Forces and moments on the rotor. Pressures on the obstacle. PIV measurements.
PoliMi	HIGE rotor in proximity to an obstacle in windy conditions	Forces and moments on the rotor. Steady and unsteady pressures on the obstacle. PIV measurements.
UoG	HIGE rotor in proximity to an obstacle without wind	Forces and moments on the rotor. Steady and unsteady pressures on the obstacle. PIV and LDA measurements

Table 1: Experimental tests

4.1 CIRA: HOGE/HIGE rotor with a loose/sling load

The external loads carried by a helicopter are typically connected in the proximity to the fuselage in order to remain in its shadow, thus avoiding unsteady aerodynamic loads induced by the main rotor wake and possible instability phenomena. Instead, for some particular missions, such as rescue operations (SAR) in adverse conditions or drop tests, these loads can be located at a larger distance from the fuselage, so that the knowledge of the wake downwash and of the forces and moments induced on the loads becomes crucial for the safety of the mission.

The CIRA test campaign aims at evaluating the effects of the main rotor wake on a sling load, in terms of aerodynamic loads and pressure distributions, in this latter condition.

The activity is ongoing.

4.1.1 Test activity

The test activity investigates firstly the characteristics of the main rotor wake several diameters downstream of the rotor disc in HOGE condition. The influence of the main rotor wake is quantified in terms of induced loads and pressure distributions on a sling load positioned at different distances from the rotor disc, while measuring the lift of the rotor. In addition, the mean load induced by the sling loads immersed in the rotor downwash wake on the rotor is measured, Figure 7. Secondly, the effect of the interaction between the rotor and the sling loads during the landing phase, when the rotor is in HIGE condition, is also evaluated, Figure 8.

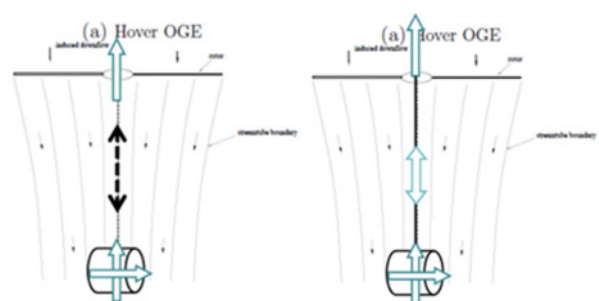


Figure 7: CIRA experimental lay-out - HOGE

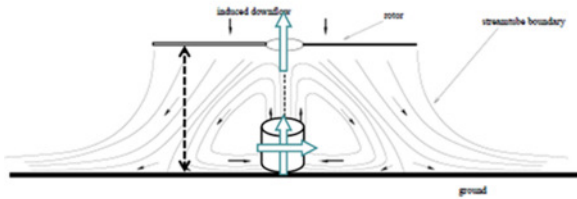


Figure 8: CIRA experimental lay-out - HIGE

The tests are being conducted in free air inside the CIRA laboratory of Testing Engineering and Methodology. The experimental campaign will make use of the R/C helicopter model Blade 450 3D RTF, equipped with a four-bladed rotor, with rectangular blades and NACA 0013 airfoil, having diameter $D = 0.72\text{m}$ and rotor speed $\Omega = 2400\text{ RPM}$, Figure 9. The forces and moments will be measured by using the six-component balance ATI Mini40 IP65. A sling load of cylindrical shape and fineness ratio 2, having length equal to 20% of the rotor diameter, is being manufactured at CIRA via Additive Manufacturing technique. The cylinder is equipped with some pressure ports for the characterization of the pressure distributions.



Figure 9: R/C helicopter Blade 450 3D RTF

4.2 ONERA: HIGE rotor in proximity to a well-shaped obstacle

ONERA developed a scaled rotor bench with the objective to investigate the interactional effects between the rotor wake and its close environment, which can be infinite or finite ground effect, or obstacles of any kind.

The activity is nearly completed and a number of related publications has been already produced and reported in the references^{[25],[26]}.

4.2.1 Test rig and obstacle model

The test rig is originally based on the commercial R/C helicopter model Sphynx 3D including a rotor head with global and cyclic control in pitch. The helicopter was strongly customised: the tail rotor and the cyclic pitch were removed; a six components balance, an external energy supply, etc. were introduced. The rotor has two rectangular

blades with NACA0012 airfoil, diameter $D = 0.71\text{m}$ and speed $\Omega = 2600\text{ RPM}$. The collective pitch was set at a fixed angle $\theta_0 = 7.5^\circ$, Figure 10.



Figure 10: R/C helicopter Sphynx 3D

The helicopter is mounted in the centre of a square-shaped courtyard as shown in Figure 11. The platform simulating a complete ground is at 1.2 m above the building floor. The walls have a parallelepiped form; they are in wood and screwed on the floor. The interior side of the walls are painted in black for the visualisations. The wall is 0.36 m high with a thickness equal to 0.30 m .

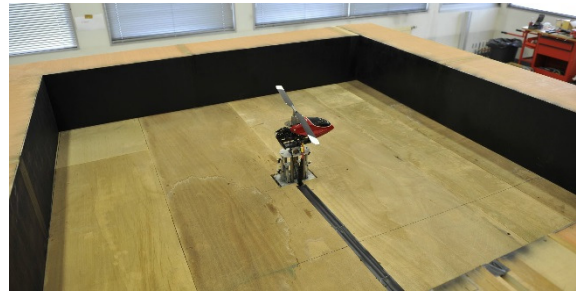


Figure 11: Helicopter mounted in a square-shaped box representing a closed courtyard

The tests were conducted in free air in a laboratory environment at ONERA Lille.

4.2.2 Test activity

Tests were realised with and without the presence of obstacles, which represent a typical town courtyard with a squared shape, in HIGE/HOGE and quasi axisymmetric conditions. The distance between the rotor and the ground was varied as indicated in Figure 12.

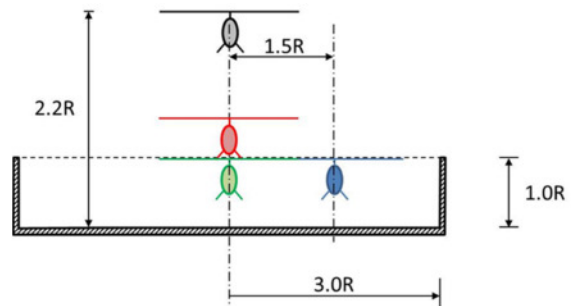


Figure 12: Layout of the ONERA test cases

The forces and moments on the rotor were measured via a 6-components balance. The acquisition of the balance

signals was done at 2 kHz during 15s with a high frequency filter at 1 kHz to eliminate the high frequencies folding.

The pressure measurements along the floor and the wall were realised by using 9 Druck PDRCR42 of 75 mbars flush-mounted on a rod alternatively inserted in the floor and in the side wall. An example is provided in Figure 13. The pressures were characterized in static (~5 sec) with a MENSOR differential sensor with a guaranteed accuracy of 0.25 Pa on the scale ± 400 Pa.

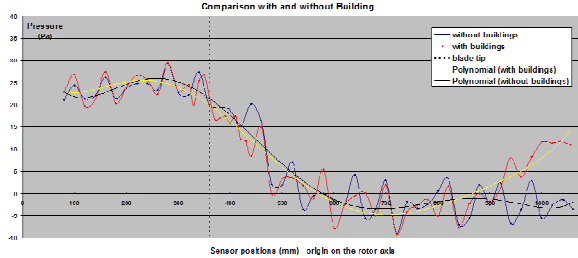


Figure 13: Pressure measurements on the ground with and without the side walls

The flow visualisation was made with a high speed video camera, a smoke generator and a laser light sheet aligned with the rotor head. Figure 14 shows an extracted image with the field of view focused on the blade tip, in direct negative colour. The rotor head appears on the right-up side. The vortices shed at the extremity of the blades are well visible and their core, generated by the centrifugation of the smoke, grows rapidly at their birth. Near the ground the flow expand radially with rebounds of the vortices at different height.

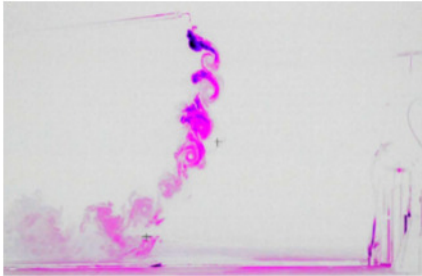


Figure 14: Smoke visualization of blade tip vortices

The Stereo-PIV measurement were made in an area located below the rotor and on the advancing blade side of the model, Figure 15. The two PIV cameras as well as the laser were synchronized with one-per-rev signal provided by a sensor on the helicopter rotor. The acquisition frequency was set at 4.8 Hz, which is equivalent to one PIV recording for nine rotor revolutions. Figure 16 shows an example from the SPIV results of the flow field in between the helicopter and the surrounding walls.

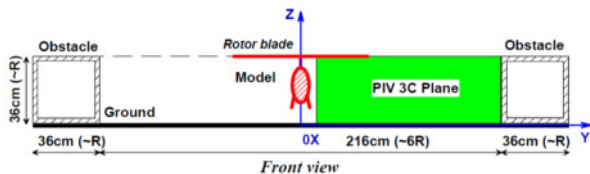


Figure 15: Configuration of the model and PIV zone

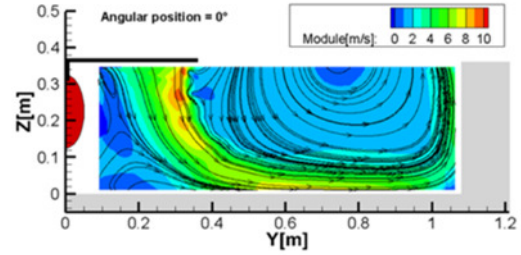


Figure 16: Module of the velocity field.

4.3 PoliMi: HIGE rotor in proximity to an obstacle in windy conditions

The wind tunnel test campaign proposed by PoliMi deals with a helicopter model hovering in close proximity to a solid obstacle, with and without natural wind, with the aim to study the mutual aerodynamic interference. A first entry for the wind-off test was carried out in a large testing environment on the side of the wind tunnel. The second test entry, comprising both wind-on ($\mu = 0.05$) and wind-off tests, was instead carried out in the large test section of the Wind Tunnel of Politecnico di Milano (GVPM), whose dimensions allowed for an even reduced interference with the surroundings.

The activity is completed and a number of related publications has been already produced and reported in the references^{[27],[28],[29],[30]}.

4.3.1 Test rig and obstacle model

The test rig consists of an in-house developed helicopter model, inspired to the MD-500, fixed to a horizontal pylon that can be moved by a system of two traversing guides so that its height from the ground and distance from the obstacle can be changed. The roll angle of the helicopter can be adjusted.

The helicopter model is powered by an on-board electric motor and is fixed to the pylon by the tail (tail rotor is not present), Figure 17.

The rotor model has four rectangular blades with NACA 0012 airfoil, and the following main characteristics:

- Diameter $D = 0.75\text{m}$;
- Chord $c = 0.032\text{m}$;
- Solidity $\sigma = 0.11$;
- Fixed collective pitch $\theta_0 = 10^\circ$;
- No cyclic pitch;
- Speed $\Omega = 2480\text{ RPM}$ (1st entry) - $\Omega = 2580\text{ RPM}$ (2nd entry)

The obstacle was provided by DLR and the main characteristics are described in section 4.5.

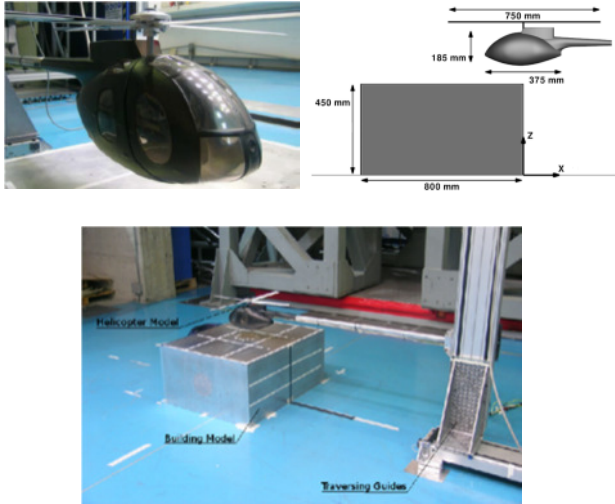


Figure 17: Helicopter model & Test Rig

4.3.2 Wind tunnel characteristics

The Wind Tunnel of Politecnico di Milano is widely used for helicopter tests thanks to the generous dimensions of its test chamber (4m x 3.84 m) and its very good flow quality. Furthermore this facility allows to use the return duct too as a quite large test chamber (13.84m x 3.84m) usually utilized for building tests. The tests of the present campaign were carried out inside this huge room as represented in Figure 18 in order to minimize the interference effect of the surroundings.



Figure 18: PoliMi GVPM experimental lay-out

4.3.3 Test activity

Several model settings, Figure 19, were tested during the campaign by changing the following three parameters:

- 1) horizontal distance from the obstacle;
- 2) height from the ground;
- 3) wind velocity.

Each combination of them defined a test configuration. A matrix, containing the lists of the configurations was defined before the start of the campaign.

The following measurements were made for each test:

- 1) forces and moments on the rotor by means of a 6-components balance (20E12A JR3 Force Torque Sensor);
- 2) steady (average values) pressures on the obstacle walls (several pressure taps linked to a PSI Pressure System);
- 3) unsteady (time history) pressures on the obstacle walls (20 Kulites XCS-093). The unsteady pressure acquisition was synchronized with the acquisition of the rotor blade azimuthal position;
- 4) PIV flow field survey downstream of the obstacle, Figure 20.

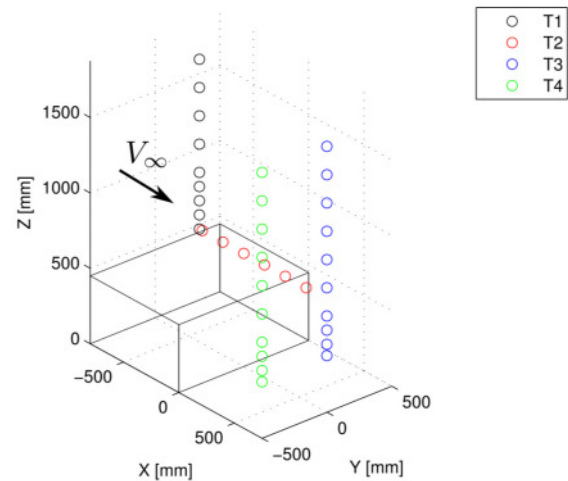


Figure 19: PoliMi measurement points

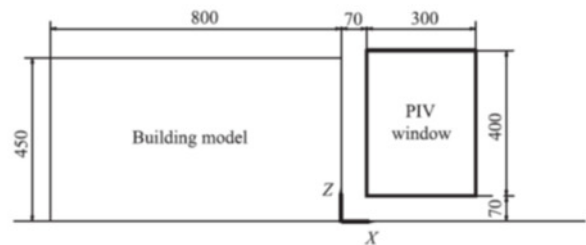


Figure 20: PIV measurements

An example of the measured pressures and PIV are illustrated in Figure 21 and Figure 22, respectively.

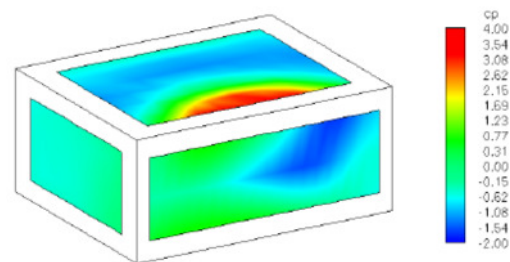


Figure 21: Example of C_p measurements on the PoliMi obstacle in wind-off conditions - $\mu = 0.05$

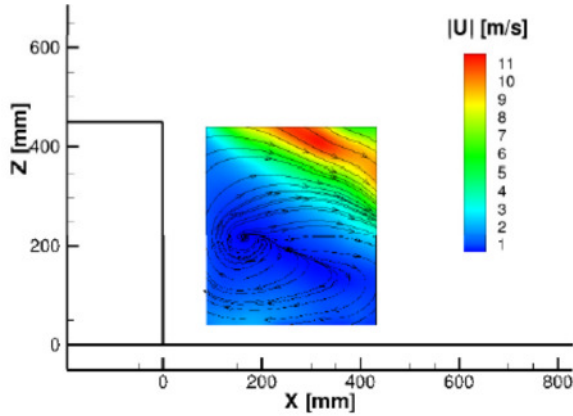


Figure 22: Example of PIV measurements on the PoliMi obstacle in wind-off conditions - $\mu = 0.05$

4.4 UoG: HIGE rotor in proximity to an obstacle without wind

The wind tunnel test campaign proposed by UoG was aimed at investigating the rotor flow in the vicinity of an obstacle. In particular, it consisted of a set of tests reproducing hovering flight conditions at different positions with respect to a cubic obstacle with side dimension equal to the rotor diameter. Two different rotor rigs were used and load measurements from the rotor, pressure measurements on the obstacle faces and velocity measurements of the air flow were gathered during the campaign.

The activity is completed and a number of related publications has been already produced and reported in the references^{[27],[29]}.

4.4.1 Test rig, obstacle model and equipment

Two simplified rotor systems available at Glasgow were used within this project: large rotor rig 1; small rotor rig 2. The notional obstacle was a simple cuboid shape, which was mounted on a load cell. In addition it was fitted with surface mounted transducers.

The main characteristics of the rigs and the obstacle are summarised in Table 2.

Characteristics	Rotor Rig 1 (Large)	Rotor Rig 2 (Small)
Obstacle size	1 m	0.3 m
Rotor diameter	1 m	0.3 m
Number of blades	4	2
Blade chord	53 mm	31.7 mm
Solidity	0.135	0.134
Collective pitch	8°	8°
Rotor speed	1200 rpm	4000 rpm

Table 2: Main features of the UoG rotor rigs.

Rotor rig 1, Figure 23, was placed in a large laboratory space with an even, flat ground extending to a 5m radius

away from the rotor centre line. It was used to carry out forces and moments and LDA measurements.

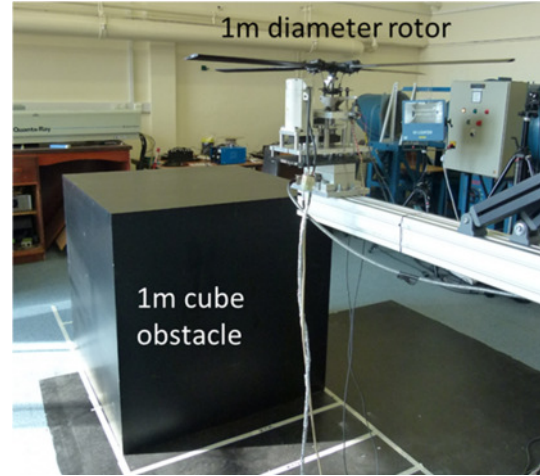


Figure 23: UoG large rotor test rig 1

Rotor rig 2, Figure 24, could be used in the same laboratory space, or it could be mounted in the UoG de Havilland wind tunnel, which has a 2.66m x 2.07m x 5.6m (W x H x L) working section. This rotor rig was used to perform Stereo-PIV and pressure measurements as well as flow visualizations.

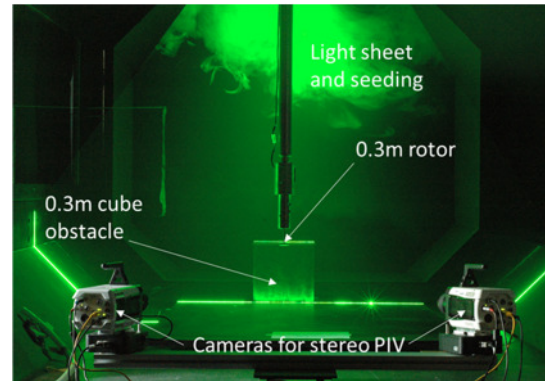


Figure 24: UoG small rotor test rig 2

4.4.2 Test activity

The matrix of the tests conducted at UoG is reported in Figure 25 where the red circles indicate the positions of the centre of the rotor with respect to the obstacle. Some conditions on planes different from the symmetry plane were also tested.

The following measurements were made for each test:

1. forces and moments generated by the rotor were measured by a 6-components AMTI MC36 model load cell mounted on the rotor rig 1. The intention to trim the rotor to zero rolling and pitching moment by varying the cyclic angle settings proved to be difficult in practice so the moments were measured for given blade settings and the changes in moment due to rotor proximity to the obstacle were recorded;

2. a 2-component LDA system mounted on a traverse system was used to measure the induced velocity on a plane 40mm above the rotor rig 1, as the distance from the ground and from the obstacle changed;
3. a ZOC valve system was used to measure the pressure on the top and side faces of the cubic obstacle. These measurements were taken by using the rotor rig 2 to provide support data for the PIV analysis in addition to the obstacle load. Some data were sampled with the rotor rig in the wind tunnel, while other cases were run in the large laboratory space;
4. The LaVision system running Davis 8 stereoscopic PIV was used to measure the flow in the region of recirculation between the obstacle and the rotor. The system was installed in the working section of the UoG de Havilland wind tunnel, and the rotor rig 2 was used for these tests.

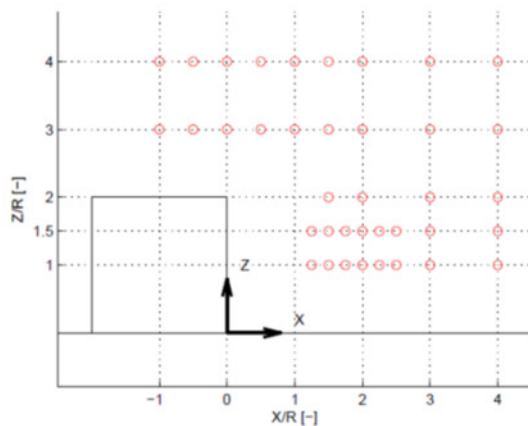


Figure 25: UoG Measurement points

An example of the measurements acquired during the test campaign is provided in Figure 26, referring to an LDA scan.

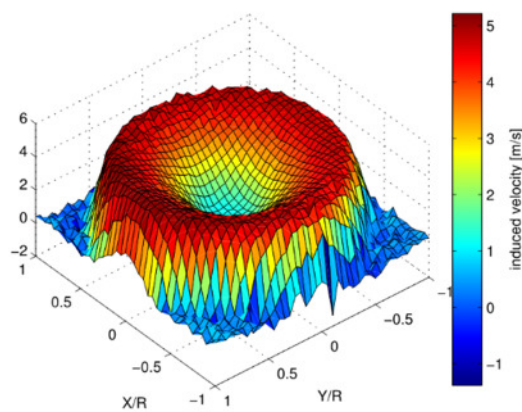


Figure 26: LDA scan over rotor disc. Inflow velocity

Smoke flow visualizations were also made and an is shown in Figure 27.

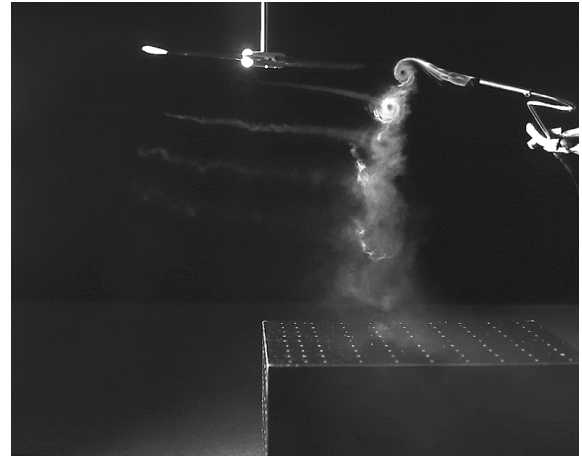


Figure 27: Smoke flow visualisation.
 $z/D = 1.93$ above the ground

4.5 DLR F20 model obstacle

A wind tunnel model, property of DLR, was used as an obstacle during the activities of the project. The DLR-F20-wind tunnel model^[31] resembles a container in model scale. The model was originally used to measure the airloads and pressure distributions in the context of a study for air dropping of containers from military transport aircraft (DLR-MiTraPor-Project), Figure 28.



Figure 28: DLR-F20-Model in DNW-NWB-Wind Tunnel, Braunschweig

The model is a cuboid with size 0.45 m x 0.8 m x 1.0 m. The cuboid is made from an aluminium frame onto which aluminium plates are fixed, Figure 29. It is instrumented with 5 Kulites and 155 pressure taps, Figure 30. The Kulites are still installed. The PSI-module has been removed but all tubes and clutches are still installed.



Figure 29: Internal layout of brick



Figure 30: Sensor installation on brick

During the HC/AG-22 experiments, the cuboid was simply laid down on the floor.

5 NUMERICAL ACTIVITIES

The numerical investigations are performed by each partner applying in-house-developed or commercial computational tools. Preliminary computations were performed with the aim to test the initial modelling capabilities of the proposed tools. Code enhancements are also carried out for those cases where an improvement of the tools capabilities was required in order to better simulate the phenomenology under investigation. All partners are currently involved in the final validation activity.

The simulations are performed by using computational methodologies, which span from the lower fidelity flight mechanics ones up to the high fidelity and sophisticated Navier-Stokes based ones, Figure 31. The numerical tools are summarized in Table 3 and described in the following.

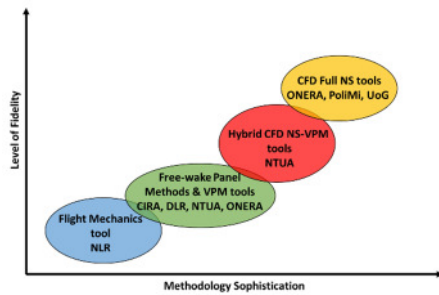


Figure 31: Numerical methodologies applied

PARTNER	CODE	METHODOLOGY	DESCRIPTION
CIRA	RAMSYS	BEM+FW	Boundary Element Method + Free Wake + Mirror Image/Surface Singularity Method
DLR	UPM	FW-PM	Unsteady free wake panel method
NLR	FLIGHTLAB	MB+FM	Multi-body + Flight Mechanics
NTUA	GENUVP	BEM+FW	Unsteady panel method + Free Wake Vortex Particle Method
	HoPFlow	Hybrid N-S	CFD Navier-Stokes method + Vortex Particle Method
ONERA	PUMA	FW	Free Wake model
	elsA	N-S	CFD Navier-Stokes method
PoliMI	Rosita	N-S	CFD Navier-Stokes method using actuator disc modelling
UoG	HMB2	CFD+FM+SD	CFD method coupled with flight mechanics module and rotor blade structural dynamics

Table 3: Numerical methodologies applied

CIRA computations are performed by RAMSYS^[32], which is an unsteady, inviscid and incompressible free-wake BEM solver, developed at CIRA, for multi-body configurations. It is based on Morino's boundary integral formulation for the solution of Laplace's equation for the velocity potential ϕ . Ground effect problems are solved by the application of a Mirror Image Method (MIM) or by using the more sophisticated Surface Singularity Method (SSM). The forces on the obstacles are evaluated by integrating the surface pressure distributions.

An example of predicted pressure distributions on the obstacle and ground surfaces is shown in Figure 32 and Figure 33.

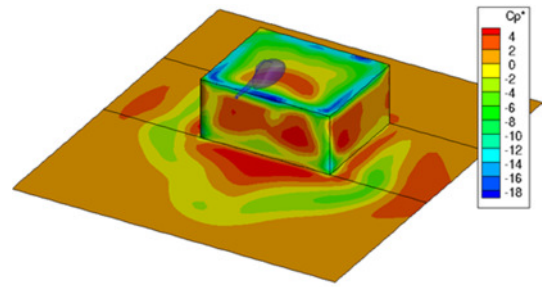


Figure 32: Cp distribution over PoliMi obstacle in wind-off conditions – $x/R = 0$; $z/R = 2$

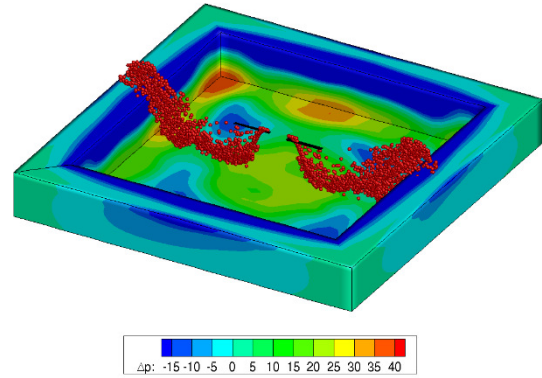


Figure 33: Cp distribution over ONERA well-shaped obstacle and ground

DLR applies the panel method UPM to study the interference effects between rotor and obstacle. UPM^[33] is an unsteady free wake panel method based on the Laplace equation. The ground and obstacles may be modelled by a panelised surface with sources/sinks. The rotor is trimmed allowing the analysis of the rotor trim state in the presence of an obstacle.

A related publication has been already produced and reported in the reference^[34].

An example of computed flowfield velocities and streamlines around the PoliMi obstacle in wind-on conditions is shown in Figure 34.

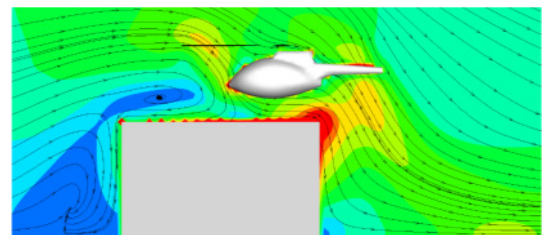


Figure 34: In-plane velocity magnitude contours and streamlines for the PoliMi obstacle in wind-on conditions at $\mu = 0.05 - x/R = -0.5$; $z/R = 2$

NLR uses the commercial tool FLIGHTLAB^[35]. It contains a panel method for the modelling of ground/walls/ship deck that is used to interact with rotor wakes. The rotor wake may be modelled by means of a simple Peters/He finite-state wake or by the more complex free vortex wake methods. The vortex wake is either prescribed or free and a time-accurate method is also available. A method for the

computation of the rotorcraft wake geometry using NURBS is also proposed for further development and implementation.

An example of computed C_p and streamlines for the ONERA well-obstacle is shown in Figure 35.

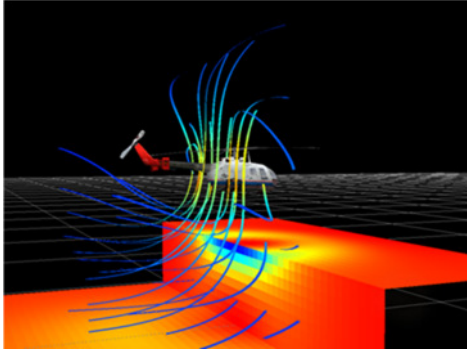


Figure 35: C_p and streamlines for the ONERA well-obstacle experimental case, full-scale dimensions with BO105

NTUA simulations are performed using two codes. The first is GENUVP^{[36],[37],[38]}, a panel code combined with a vortex particle approximation of the wake. The code uses a multi-block MPI-enabled Particle Mesh solver for the wake evolution and tree algorithms for the panel part. The wake is generated along prescribed lines such as trailing edges of blades and corner lines of bluff bodies. The second code is HoPFlow^[39], a fully coupled hybrid code that combines a URANS un-structured compressible solver close to solid boundaries with an overlapped Particle Mesh Lagrangian solver using compressible particle approximations. The particles carry mass, vorticity, dilatation and energy while their volume is varying in order to take into account flow compressibility. In the case of independently solid bodies (rotor blades and fuselage) separate grid are introduced for each one.

A related publication has been already produced and reported in the reference^[40].

An example of wake development modelling for the PoliMi obstacle in wind-off conditions is shown in Figure 36.

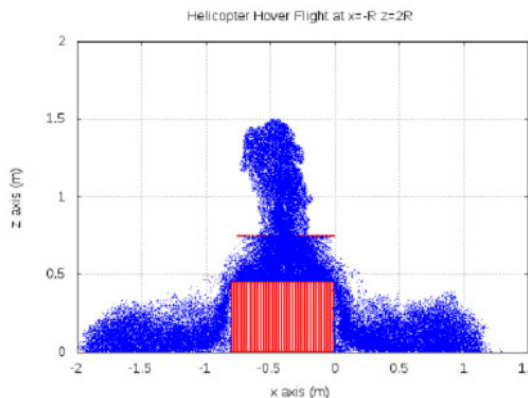


Figure 36: Wake development for the PoliMi obstacle in wind-off conditions - $x/R = -1$; $z/R = 2$

ONERA computations are performed using two different tools. The first one is the PUMA code^{[41],[42]} developed at

ONERA based on the same approach than the MINT code, for the free wake model and extended with a multi-body module and the Multilevel Fast Multipole Method. To take into account for any kind of obstacle geometry, specific developments are implemented in the context of this GARTEUR. The second tool is the elsA code^[43], an unsteady Navier-Stokes code able to simulate complete helicopter configuration taking into account any kind of obstacle geometry.

A related publication has been already produced and reported in the reference^[26].

An example of wake development and flow field velocity predictions by PUMA and elsA codes is shown in Figure 37 and Figure 38.

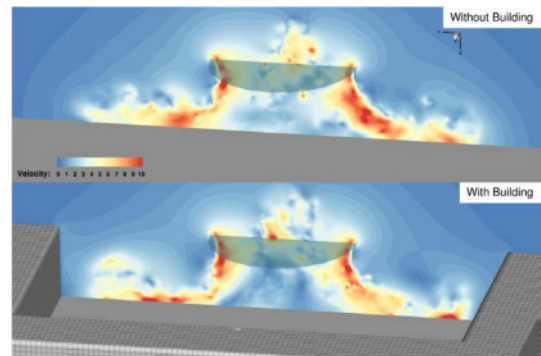


Figure 37: Lifting-line + free wake modelling of the wake development for the ONERA obstacle

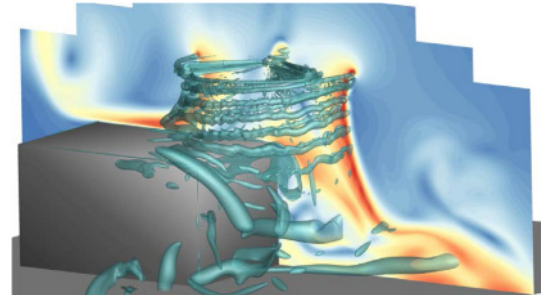


Figure 38: N-S wake modelling for the PoliMi obstacle in wind-off conditions - $x/R = 1$; $z/R = 2$

PoliMi adopted computational scheme is a coupled approach making use of the ROSITA^{[44],[45]} Navier-Stokes (NS) solver and a Blade Element (BE) approximation. The coupling is made by means of an actuator disk: the loads computed with the BE approach are introduced in the NS computation through the disk actuator, then from the NS solution the velocity on the disk are obtained and used again for the load evaluation by means of BE. The iterations continue until convergence.

The CFD code ROSITA numerically integrates the unsteady compressible Reynolds Averaged Navier-Stokes (RANS) equations, coupled with the one-equation turbulence model by Spalart-Allmaras. Multiple moving multi-block grids can be employed to build an overset grid system using the Chimera technique. The equations are discretised in space by means of a cell-centred finite-volume implementation of the Roe's scheme. The Gauss theorem and a cell-centred discretisation scheme are used to compute the viscous terms of the equations. Time

advancement is carried out with a dual-time formulation, employing a 2nd order backward differentiation formula to approximate the time derivative and a fully unfactored implicit scheme in pseudo-time.

A related publication has been already produced and reported in the reference^[28.].

An example of computed flowfield velocities and streamlines is shown in Figure 39 and a comparison between measured and computed PIVs is given in Figure 40.

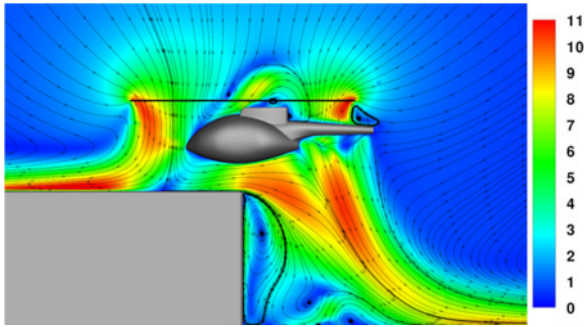


Figure 39: In-plane velocity magnitude contours and streamlines for the PoliMi obstacle in wind-off conditions - $x/R = 0$; $z/R = 2$

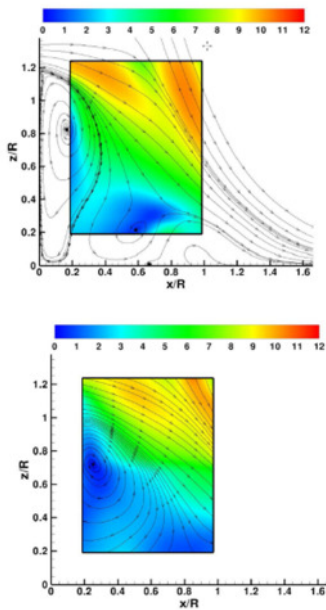


Figure 40: Comparison between computed (top) and measured (bottom) flow-field. PoliMi obstacle in wind-off conditions - $x/R = 0$; $y/R = 0$, $z/R = 2$.

UoG employs the Helicopter Multi-Block Method HMB2 code^{[47.],[48.],[49.],[50.]}, that has rotor-modelling capability using either resolved blades or actuator disk models. The solver uses RANS/URANS methods on overset grids and fast implicit algorithms to speed-up convergence.

A related publication has been already produced and reported in the reference^[46.].

An example of the N-S wake modelling and streamlines evaluation is shown in Figure 41 while Figure 42 illustrates

a comparison between measured and computed C_p on the obstacle surface.

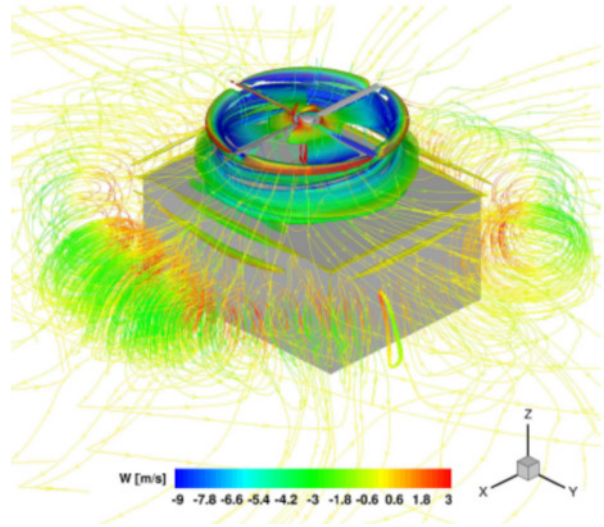


Figure 41: N-S wake modelling and streamlines for the PoliMi obstacle in wind-off conditions - $x/R = -1$; $z/R = 2$

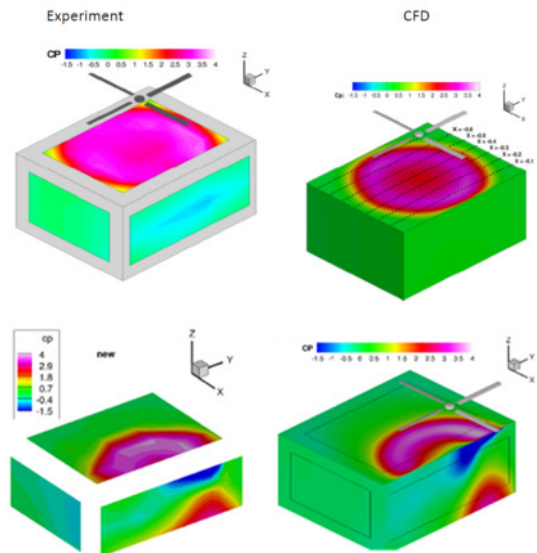


Figure 42: N-S C_p distribution for the PoliMi obstacle in wind-off conditions - $x/R = -1$; $z/R = 2$ (top) and $x/r=0, z/R=2$ (bottom)

6 CONCLUSIONS

The present paper described the objectives and the structure of the GARTEUR Action Group HC/AG-22 basic research project dealing with the evaluation of forces on obstacles in rotor wake. The project, started in November 2014 and has a duration of three years with the conclusion planned for October 2017.

The activities were structured in four work packages the main ones being represented by experimental activities and numerical investigations.

The experimental activities consisted of four low-budget wind tunnel test campaigns, complementary to each other,

conducted in the CIRA, ONERA, PoliMi and UoG test facilities, and aimed at analysing, with a wider and deeper insight, different aspects of the phenomenology. All campaigns, with the exception of the CIRA one, were concluded.

All partners were also involved in numerical investigations during which in-house developed or commercial computational tools were applied. Preliminary computations were performed with the aim to test the initial modelling capabilities of the proposed tools. Code enhancements are also carried out for those cases where an improvement of the tools capabilities was required in order to better simulate the phenomenology under investigation. All partners are currently involved in the final validation activity.

Finally, a consistent dissemination activity is promoted by the project with about ten papers presented at conferences or published on relevant scientific journals.

7 REFERENCES

- [1.] Woo, H.G.C., Peterka, J.A., Cermak, J.E., "Wind-Tunnel Measurements in the Wake of Structures," Doc. NASA CR-2806, March 1977;
- [2.] Janovsky, R., Behr, R., "Flight Testing and Test Instrumentation of PHOENIX," proceedings of the Fifth European Symposium on Aerothermodynamics for Space Vehicles (ESA SP-563), Cologne, Germany, Nov. 8-11, 2004;
- [3.] NASA Dryden Flight Research Center, <http://www.nasa.gov/centers/dryden/news/ResearchUpdate/X40A/>;
- [4.] NASA Dryden Flight Research Center Photo Collection, <http://www.dfrc.nasa.gov/gallery/photo/index.html> - Photo Nr. EC01-0107-01;
- [5.] Rufolo, G.C., Gallego Sanz, J.M., Di Vita, G., Valenzano, G., Becchio, V., Ullio, R., D'Amico, J., Marino, G., Guidotti, G., Vernillo, P., Iafrati, A., "Testing the Robustness of the Descent and Recovery Phase of ESA's Intermediate Experimental Vehicle," presented at the 63rd International Astronautical Congress, Naples, Italy, Oct. 1-5, 2012;
- [6.] Tattersall, P., Albone, C.M., Soliman, M.M., Allen, C.B., "Prediction of Ship Air Wakes over Flight Decks Using CFD," presented at the RTO AVT Symposium on "Fluid Dynamics Problems of Vehicles Operating near or in the Air-Sea Interface," Amsterdam, NL, Oct. 5-8, 1998;
- [7.] Taghizad, A., Verbeke, C., Desopper, A., "Aerodynamic Perturbations Encountered by a Helicopter Landing on a Ship – Effects of Helicopter Flight Dynamics," presented at the RTO AVT Symposium on "Fluid Dynamics Problems of Vehicles Operating near or in the Air-Sea Interface," Amsterdam, NL, Oct. 5-8, 1998;
- [8.] Lee, R.G., Zan, S.J., "Wind Tunnel Testing of a Helicopter Fuselage and Rotor in a Ship Airwake," presented at the 29th European Rotorcraft Forum, Friedrichshafen, Sept. 16-18, 2003;
- [9.] Rajagopalan, G., Niazi, S., Wadcock, A.J., Yamauchi, G.K., Silva, M.J., "Experimental and computational Study of the Interaction Between a Tandem-Rotor Helicopter and a Ship," presented at the American Helicopter Society 61st Annual Forum, Grapevine, TX, USA, June 1-3, 2005;
- [10.] Alpmann, E., Long, L.N., Bridges, D.O., Horn, J.H., "Fully-Coupled Simulations of the Rotorcraft / Ship Dynamic Interface," presented at the AHS International 63rd Annual Forum & Technology Display, Virginia Beach, VA, USA, May 1-3, 2007;
- [11.] Crozon, C., Steijl, R., Barakos, G.N., "Numerical Studies of Rotors in Ship Airwake," presented at the 39th European Rotorcraft Forum, Moscow, Sept. 3-6, 2013;
- [12.] Quinliven, T.A., Long, K.R., "Rotor Performance in the Wake of a Large Structure," presented at the American Helicopter Society 61st Annual Forum, Grapevine, TX, USA, June 1-3, 2005;
- [13.] Timm, G.K., "Obstacle-Induced Flow Recirculation," Journal of the American Helicopter Society, Vol.10, N.4, 1965;
- [14.] Iboshi, N., Itoga, N., Prasad, J.V.R., Sankar, L.N., "Ground Effect of a Rotor Hovering above a Confined Area," presented at the American Helicopter Society 64th Annual Forum, Montreal, Canada, Apr. 29-May 1, 2008;
- [15.] Polsky, S.A., Wilkinson, C.H., "A Computational Study of Outwash for a Helicopter Operating Near a Vertical Face with Comparison to Experimental Data," presented at the AIAA Modeling and Simulation Technologies Conference, Chicago, Illinois, USA, August 10-13, 2009;
- [16.] Lusiak, T., Dziubinski, A., Szumanski, K., "Interference Between Helicopter and its Surroundings, Experimental, and Numerical Analysis," Task Quarterly 13, Nr.4, pgs. 379-392, 2010;
- [17.] Gabel, R., Wilson, J.G., "Test Approaches to External Sling Load Instabilities," Journal of the American Helicopter Society, Vol.13 Nr.3, July, 1968;
- [18.] Prosser, D.T., Smith, M.J., "Navier-Stokes-Based Dynamic Simulations of Sling Loads," presented at the 54th AIAA/ASME/ASCE/AHS/ASC Structures, Structural Dynamics, and Materials Conference, Boston, USA, Apr. 8-11, 2013;
- [19.] Theron, J.N., Gordon, R., Rosen, A., Cicolani, L., Duque, P.N., Halsey, R.H., "Simulation of Helicopter Slung Load Aerodynamics: wind tunnel validation of two computational fluid dynamics codes," presented at the 36th AIAA Fluid Dynamics Conference and Exhibit, San Francisco, USA, June 5-8, 2006;
- [20.] Leese, G.W., "UH-1H Downwash Velocity Measurements," U.S. Army Engineer Waterways Experiment Station, AD-A034 667, Aug., 1972;
- [21.] Leese, G.W., Knight, I.T., "Helicopter Downwash Data," U.S. Army Engineer Waterways Experiment Station, AD-780 754, June, 1974;
- [22.] Visingardi, A., "Forces on Obstacles in Rotor Wake - Terms of Reference for the GARTEUR Action Group HC/AG-22 – Vsn. 1," Nov. 2014;

- [23.] Gent, R.W., "Pilot Paper for Wake Modelling in the Presence of Ground Obstacles", GARTEUR GoR-HC, AG17, 2006;
- [24.] Filippone, A., and AG17 partners, "GARTEUR HC/AG-17 Helicopter Wakes Models in the Presence of Ground Obstacles," report GARTEUR HC/AG-17 TP-174, Apr. 2012;
- [25.] Paquet, J.B., Bourez, J.P., Morgand, S., "Formulation of Aerodynamic Forces on helicopters in non-uniform flow with scale model tests: ground effects," presented at the 49th International Symposium of Applied Aerodynamics, Lille, France, 24-26 Mar. 2014;
- [26.] Gallas, Q., Boisard, R., Monnier, J.-C., Gilliot, A., Pruvost, J., "Experimental and numerical investigation of the aerodynamic interactions between a stationary helicopter and surrounding obstacles," presented at the 43rd European Rotorcraft Forum, Milan, Italy, 12-15 Sept. 2017;
- [27.] Zagaglia, D., Giuni, M., Green, R.B., "Rotor-Obstacle Aerodynamic Interaction in Hovering Flight: An Experimental Survey," presented at the AHS 72nd Annual Forum, West Palm Beach, (FL) USA, 17-19 May 2016;
- [28.] Zagaglia, D., Gibertini, G., Droandi, G., Antoniazza, P., Oregio Catelan, A., "CFD Assessment of the Helicopter and Ground Obstacles Aerodynamic Interference," presented at the 42nd European Rotorcraft Forum, Lille, France, Sept. 5-8, 2016;
- [29.] Zagaglia, D., Gibertini, G., Giuni, M., Green, R., "Experiments on the Helicopter-Obstacle Aerodynamic Interference in Absence of External Wind," presented at the 42nd European Rotorcraft Forum, Lille, France, Sept. 5-8 2016;
- [30.] Zagaglia, D., Gibertini, G., Campanardi, G., Grassi, D., Zanolli, A., "Helicopter-Obstacle Aerodynamic Interaction in Windy Conditions," presented at the 43rd European Rotorcraft Forum, Milan, Italy, 12-15 Sept. 2017;
- [31.] Bier, N., "Wind Tunnel Measurements of a Cuboid External Load Model," presented at the 41st European Rotorcraft Forum, Munich, Germany, 1-4 Sept. 2015;
- [32.] Visingardi, A., D'Alascio, A., Pagano, A., Renzoni, P., "Validation of CIRA's Rotorcraft Aerodynamic Modelling SYStem with DNW Experimental Data," presented at the 22nd European Rotorcraft Forum, Brighton, UK, 16-19 Sept. 1996;
- [33.] Yin, J., "Main Rotor and Tail Rotor Blade Vortex Interaction Noise under the Influence of the Fuselage", presented at the 38th European Rotorcraft Forum, Amsterdam, The Netherlands, 4-7 Sept. 2012;
- [34.] Schmid, M., "Simulation of Helicopter Aerodynamics in the Vicinity of an Obstacle using a Free Wake Panel Method," presented at the 43rd European Rotorcraft Forum, Milan, Italy, 12-15 Sept. 2017;
- [35.] Advanced Rotorcraft Technology, Inc, "FLIGHTLAB Software," www.flightlab.com;
- [36.] Voutsinas, S.G., "Vortex Methods in Aeronautics: How to make things work," International Journal of Computational Fluid Dynamics, Vol. 20, No 1, 2006;
- [37.] Huberson, S., Voutsinas, S.G., "Particles and Grid," Computers & Fluids, 31 pp 607-625, 2002;
- [38.] Voutsinas, S.G., Visingardi, A., Yin, J., Arnaud, G., Falchero, D., Dummel, A., Pidd, M., Prospathopoulos J., "Aerodynamic Interference in Full Helicopter Configurations and Assessment of Noise Emission: Pre-Test Modelling Activities for the Helinovi Experimental Campaign," presented at the 31st European Rotorcraft Forum, Florence, Italy, 13-15 Sept. 2005;
- [39.] Papadakis, G., Voutsinas, S.G. "In view of accelerating CFD computations through coupling with vortex particle approximations," Journal of Physics: Conference Series 524, 2014;
- [40.] Theologos, A., Riziotis, V.A., Voutsinas, S.G., "Rotorcraft flight in interaction with obstacles," presented at the 43rd European Rotorcraft Forum, Milan, Italy, 12-15 Sept. 2017;
- [41.] Lebouar G., Costes M., Leroy-Chesneau A., Devinant P., "Numerical simulations of unsteady aerodynamics of helicopter rotor in maneuvering flight conditions" Aerospace Science and Technology, vol. 8, pp. 11-25, 2004;
- [42.] Rodriguez B., "Blade Vortex Interaction and Vortex Ring State captured by a fully time marching unsteady wake model coupled with a comprehensive dynamics code," HeliJapan, Saitama, Japan, Nov. 2010;
- [43.] Cambier L., Heib S., Plot S., "The Onera elsA CFD software: input from research and feedback from industry", Mechanics & Industry / Volume 14 / Issue 03 / January 2013, pp 159-17;
- [44.] Biava, M., "RANS computations of rotor/fuselage unsteady interactional aerodynamics," PhD Thesis, Politecnico di Milano
- [45.] Biava, M., Pisoni, A., Saporiti, A., Vigeveno, L., "Efficient rotor aerodynamics predictions with a Euler method," presented at the 29th European Rotorcraft Forum, Friedrichshafen, Germany, Sept. 16-18 2003;
- [46.] Chirico, G., Vigeveno, L., Barakos, G.N., "Numerical Modelling of the Aerodynamic Interference between Helicopter and Ground Obstacles," presented at the 41st European Rotorcraft Forum, Munich, Germany, Sept. 1-4 2015;
- [47.] Johnson, G. and Barakos, G.N., "Optimizing Rotor Blades with Approximate British Experimental Rotor Programme Tips", AIAA Journal of Aircraft, 2014. doi: 10.2514/1.C032042;
- [48.] Woodgate, M. and Barakos, G.N., "Implicit CFD Methods for Fast Analysis of Rotor Flows", AIAA Journal, **50**(6), 1217-1244, June 2012, DOI: 10.2514/1.J051155;
- [49.] Steijl, R. and Barakos G.N., "CFD Analysis of Complete Helicopter Configurations Lessons Learnt from the GOAHEAD Project", *Aerospace Science and Technology*, **19**(1), 58-71, June 2012, DOI: 10.1016/j.ast.2011.01.007;
- [50.] Brocklehurst, A., and Barakos, G.N., "A Review of Helicopter Rotor Blade Tip Shapes," Progress in Aerospace Sciences, **56**, 35-74, January 2013; DOI: 10.1016/j.paerosci.2012.06.003.